Advances in Adaptive Data Analysis
Vol. 1, No. 1 (2009) 43–59

World Scientific
www.worldscientific.com

SAMPLING EFFECTS ON THE EMPIRICAL MODE DECOMPOSITION

GABRIEL RILLING* and PATRICK FLANDRIN†

Laboratoire de Physique (UMR 5672 CNRS)
École normale supérieure de Lyon
46 allée d'Italie, 69364 Lyon Cedex 07 France
**gabriel.rilling@ens-lyon.fr*
†*patrick.flandrin@ens-lyon.fr*

Standard exposition of Empirical Mode Decomposition (EMD) is usually done within a continuous-time setting whereas, in practice, the effective implementation always operates in discrete-time. The purpose of this contribution is to summarize a number of results aimed at quantifying the influence of sampling on EMD. The idealized case of a sampled pure tone is first considered in detail and a theoretical model is proposed for upper bounding the approximation error due to finite sampling rates. A more general approach is then discussed, based on the analysis of the nonlinear operator that underlies the EMD (one step) sifting process. New explicit, yet looser, bounds are obtained this way, whose parameters can be estimated directly from the analyzed signal. Theoretical predictions are compared to simulation results in a number of well-controlled numerical experiments.

Keywords: EMD; sampling.

1. Introduction

In most expositions of "Empirical Mode Decomposition" (EMD), it is implicitly assumed that the considered signals are given in *continuous-time* and, indeed, the rationale underlying EMD is more intuitive this way.[1] In practice however, EMD is usually implemented in *discrete-time* and applied to digital time series, either because the analyzed data is intrinsically discrete, or because it results from the sampling of some underlying continuous-time process. Considering a continuous-time signal, the sampling step which is required prior applying EMD is expected to affect the resulting decomposition in some way, and it is therefore the purpose of this paper to address some of the issues raised by sampling in the context of EMD, so as to help in a well-controlled (and, hopefully, robust) use of the technique in practical situations. More precisely, the paper is organized as follows. Section 2 provides a detailed analysis of the influence of sampling in the simplified case of a single tone. Under a number of assumptions that are critically examined, an upper bound is derived for the approximation due to finite sampling rates, and the relevance of the theoretical model is supported by numerical simulations. The analysis is further

generalized beyond tones in Sec. 3, on the basis of a study of the elementary sifting operator involved in the EMD. This results again in a predicted bound for the error, that it shown to depend on parameters that can be estimated from the data. A set of numerical simulations with synthetic signals is then performed for assessing the performance of the theoretical upper bound model.

2. EMD of a Tone

Let us start with the simplest example of a continuous-time tone, i.e., a waveform $x(t)$ defined as the sinusoidal, unit period, signal

$$x(t) = \cos 2\pi t. \tag{1}$$

In this idealized situation, the analyzed signal fulfils — by construction — all the requirements for being an "Intrinsic Mode Function" (IMF),[1] and EMD is in this case expected to act as the identity operator, with the signal itself as the unique output IMF and no residual. Whereas this interpretation obviously holds true in continuous-time, it turns out that the picture is dramatically changed when sampling enters the play. In fact, EMD is constructed on signal extrema, and the extrema of a sampled signal generally differ from those of its continuous-time counterpart: it follows that the local mean (defined as the mean of the envelopes interpolating the extrema) may present some sampling related artefacts, as illustrated in Fig. 1.

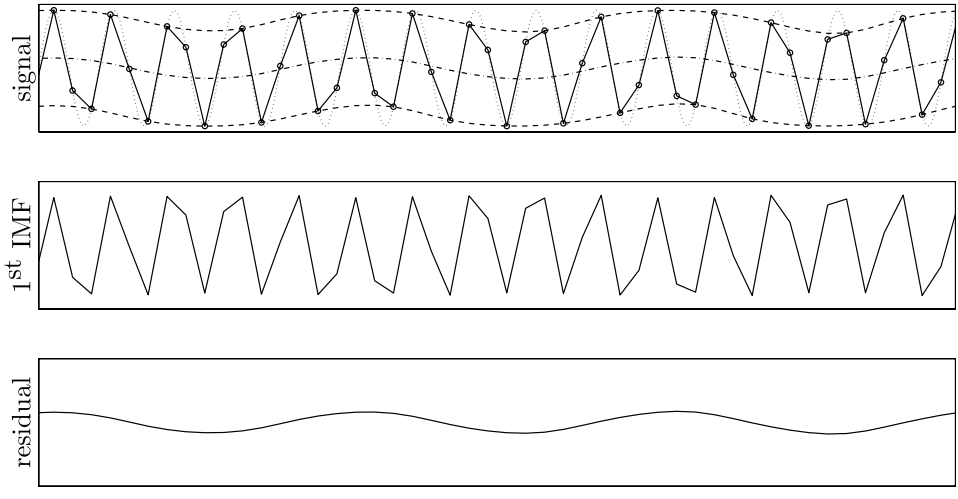

Fig. 1. EMD of a tone — Qualitative influence of sampling. The analyzed tone is plotted in dotted line and its sampled version in solid line (top diagram). Due to the finite (though admissible in Shannon's sense) sampling rate, the upper and lower envelopes (dashed lines) as well as their local mean (dash–dot line) are oscillating. As a result of this oscillation, the first extracted IMF (middle diagram) does not exhaust the description of the signal as it would be expected for a continuous-time tone, and a nonzero residual oscillation is introduced (bottom diagram).

2.1. *Sampling error as a function of the sampling frequency*

In order to evaluate the influence of sampling, we introduce sampled versions of (1) as

$$x_{f_s,\varphi}[n] = x\left(\frac{n}{f_s} + \varphi\right) = \cos\left(\frac{2\pi}{f_s}n + 2\pi\varphi\right) \tag{2}$$

with $n \in \mathbb{Z}$, where f_s and φ stand for the sampling frequency and phase, respectively. Since the original signal (1) is already an IMF, we then propose to evaluate the influence of the sampling parameters f_s and φ by using as an error criterion the simple (l_1) discrepancy function

$$e_x(f_s,\varphi) = \frac{\sum_{n=1}^{N} |x_{f_s,\varphi}[n] - d_{f_s,\varphi}[n]|}{\sum_{n=1}^{N} |x_{f_s,\varphi}[n]|}, \tag{3}$$

where $d_{f_s,\varphi}[n]$ stands for the first IMF computed from the discrete-time version (2) of the continuous-time tone (1). We will also define and use another quantity $\bar{e}_x(f_s)$, which is the phase averaged version of $e_x(f_s,\varphi)$:

$$\bar{e}_x(f_s) = \mathbb{E}_\varphi\{e_x(f_s,\varphi)\} = \int_0^1 e_x(f_s,\varphi)\, d\varphi, \tag{4}$$

with φ a random variable uniformly distributed over the interval $[0,1)$.

2.2. *Bounding the sampling error*

The influence of sampling on the EMD of a pure tone has already been partly considered in previous publications,[2–5] and it has been observed (from simulation experiments) that the criterion (3) admits an upper bound inversely proportional to the square of the sampling frequency.[a] The purpose of this section is to justify this observed behavior. More precisely, we will prove that

$$e_x(f_s,\varphi) \leq \frac{\pi}{4}\left(1 - \cos\frac{\pi}{f_s}\right) \leq \frac{\pi^3}{8f_s^2}, \tag{5}$$

the first bound being furthermore tight when $\varphi = 0$ and $f_s = 2k+1, k \in \mathbb{N}$.

In order to do so, we will have to make some assumptions, which consist of the following three approximations:

1. The upper envelope interpolating the maxima takes values between the smallest maximum and 1. Similarly, the lower envelope takes values between -1 and the greatest minimum.
2. The first IMF is obtained through a unique sifting step.
3. The l_1-norm of $x_{f_s,\varphi}[n]$ is exactly $2N/\pi$.

[a]In fact, the experiments conducted in Refs. 2 and 3 adopted a reversed perspective as compared to the approach followed here: the sampling frequency was indeed kept fixed (and arbitrarily set to unity) and the frequency of the analyzed tone was varied. It followed that the error measure was evaluated as a function of the tone frequency, with an observed upper bound proportional to its square.

The first approximation allows us to control the value of the envelopes by just considering the extrema. Actually, this approximation can also be exact depending on the interpolation used to compute the envelopes. As a matter of fact, this is the case for linear interpolation and for the built-in `MATLAB pchip` (a.k.a. `cubic`) interpolation. Unfortunately, it is only an approximation for the cubic spline interpolation, which is by far the most commonly used. Nevertheless, this approximation holds well in the specific case of sinusoidal signals.

The second approximation is a bit more questionable. In fact, it generally takes more than one sifting step to obtain an admissible IMF. However, the first sifting step is always the most important one, and the following steps just improve slightly the final result. It has nevertheless to be noticed that this may not be the case for any input signal: for some signals indeed, the first sifting step can reveal new extrema and, therefore, the next sifting step may be as important as the first one. In the specific case of sinusoidal signals, there are however no new extrema revealed by any sifting step, and neglecting the sifting steps after the first one is therefore a reasonable hypothesis.

Finally, the third approximation is nearly exact for almost all sampling frequencies provided there is a large number of periods in the signal. The only exceptions occur for sampling frequencies that are simple rational numbers but, even in these cases, the discrepancy is rather small.

Assuming that the three above approximations hold, the proof of (5) proceeds as follows. Using first the third hypothesis, we can write (3) as

$$\begin{aligned} e_x(f_s,\varphi) &= \frac{\sum_{n=1}^{N} |x_{f_s,\varphi}[n] - d_{f_s,\varphi}[n]|}{\sum_{n=1}^{N} |x_{f_s,\varphi}[n]|} \\ &= \frac{\pi}{2N} \sum_{n=1}^{N} |m_{f_s,\varphi}[n]| \,, \end{aligned} \tag{6}$$

where $m_{f_s,\varphi}[n]$ is the local mean of $x_{f_s,\varphi}[n]$, which is also the mean of the envelopes $e_{\min}[n]$ and $e_{\max}[n]$ thanks to the second hypothesis. Using then the first hypothesis, we know that $e_{\max}[n]$ is positive and $e_{\min}[n]$ negative. Thus,

$$\begin{aligned} |m_{f_s,\varphi}[n]| &= \left| \frac{e_{\max}[n] + e_{\min}[n]}{2} \right| \\ &= \frac{||e_{\max}[n]| - |e_{\min}[n]||}{2} \\ &\leq \frac{1-\alpha}{2}, \end{aligned}$$

where $-\alpha$ is an upper bound for the values of the minima or, alternatively, α is a lower bound for the maxima. The value of α is rather easy to obtain as it corresponds to the case where two consecutive sampling points hit the continuous-time sinusoid symmetrically with respect to one of its extrema. We get therefore $\alpha = \cos(\pi/f_s)$

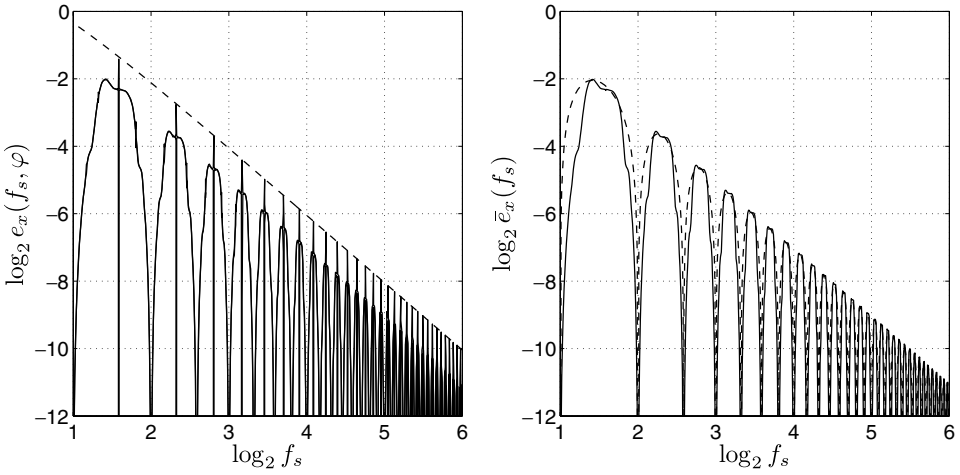

Fig. 2. EMD of a tone — Quantitative influence of sampling. The left diagram displays (solid lines) the actual maximum and minimum (with respect to the phase) error (3) as a function of the sampling frequency in the case of a tone with $N = 2048$ data points, the superimposed dashed line corresponding to the (tightest) upper bound given by (5). The right diagram displays the same way (solid line) the associated phase-averaged error (4), the superimposed dashed curve corresponding to the model (10).

and, using finally the common formula "$\cos u \geq 1 - u^2/2$," we obtain the last part of the desired result (5).

The obtained upper bound is furthermore reached for sampling frequencies $f_s = 2k + 1, k \in \mathbb{N}$ and phase $\varphi = 0$. In this case indeed, the upper and lower envelopes are constants with respective values 1 and $-\cos(\pi/f_s)$, and the $\pi^3/8$ coefficient in the f_s^{-2} bound is thus optimal. This concludes the proof.

Figure 2 (left diagram) illustrates the behavior of the actual error (3) as a function of the sampling frequency, as well as the effectiveness of the upper bound (5).

2.3. *A model for the phase-averaged sampling error*

Based on the same set of hypotheses, we can propose for the phase-averaged sampling error a model which is closer to the observed experimental results. Unlike the previous analysis, this model does not give, *per se*, an upper bound for $\bar{e}_x(f_s)$ but rather an order of magnitude for it and, thus, for $e_x(f_s, \varphi)$. An advantage of this new model (which, as for the upper bound model, is only based on some considerations about the extrema of the sampled signal) is however its ability to describe the overall shape of the sampling error and, in particular, to justify its decay around sampling frequencies that match even integers.

Let us first notice that the sampling phase being a random variable uniformly distributed over $[0, 1)$, the process $x_{f_s,\varphi}[n]$ is stationary. If we ignore boundary conditions issues, we can assume that $d_{f_s,\varphi}[n]$ and $m_{f_s,\varphi}[n]$ are stationary processes

as well. Therefore, using (6), we can simplify the expression of $\bar{e}_x(f_s)$ and get, for any n

$$\bar{e}_x(f_s) = \frac{\pi}{2}\mathbb{E}_\varphi\left\{|m_{f_s,\varphi}[n]|\right\}. \tag{7}$$

The next step is therefore to estimate locally the value of the local mean of the signal. To this end, the main idea is to approximate the values of the envelopes by the values of the nearest extrema. It follows that the absolute value of the local mean can be approximated by

$$|m_{f_s,\varphi}[n]| \approx \frac{1}{2}\left|\cos\left(\frac{2\pi}{f_s}n_{\max} + 2\pi\varphi\right) + \cos\left(\frac{2\pi}{f_s}n_{\min} + 2\pi\varphi\right)\right|,$$

where $n_{\max}$ (resp. $n_{\min}$) refers to the index of the nearest maximum (resp. minimum).

Knowing that a maximum of the sampled signal is distant from the corresponding maximum of its continuous-time counterpart by at most half a sampling period, there exists necessarily an integer k such that

$$\varphi_{\max} \equiv \frac{n_{\max}}{f_s} + \varphi - k \in \left[-\frac{1}{2f_s}, \frac{1}{2f_s}\right].$$

Moreover, if φ varies uniformly over $[0,1)$, so does $\varphi_{\max}$ over $[-1/(2f_s), 1/(2f_s))$ and, therefore

$$\mathbb{E}_\varphi\left\{|m_{f_s,\varphi}[n]|\right\} \approx \frac{1}{2}\mathbb{E}_\psi\left\{\left|\cos\psi + \cos\left(\frac{2\pi\tilde{n}(\psi)}{f_s} + \psi\right)\right|\right\}, \tag{8}$$

where ψ is a random variable uniformly distributed over $[-\pi/f_s, \pi/f_s)$ and $\tilde{n}(\psi) > 0$ refers to the index of the first minimum of $\cos(2\pi n/f_s + \psi)$. If we let K be the integer part of $f_s/2$ and $\tilde{\psi} = \pi - (2K+1)\pi/f_s$, we can express $\tilde{n}(\psi)$ as follows:

$$\tilde{n}(\psi) = \begin{cases} K & \text{if } \psi > \tilde{\psi}; \\ K+1 & \text{if } \psi < \tilde{\psi}. \end{cases}$$

Replacing $\tilde{n}(\psi)$ by its value in (8) yields

$$\begin{aligned}
\mathbb{E}_\varphi\{|m_{f_s,\varphi}|\} &\approx \frac{f_s}{4\pi}\int_{-\pi/f_s}^{\pi/f_s}\left|\cos\psi + \cos\left(\frac{2\pi\tilde{n}(\psi)}{f_s} + \psi\right)\right| d\psi, \\
&\approx \frac{f_s}{4\pi}\left[\int_{\tilde{\psi}}^{\pi/f_s}\left|\cos\psi + \cos\left(\frac{2\pi K}{f_s} + \psi\right)\right| d\psi\right. \\
&\quad \left. + \int_{-\pi/f_s}^{\tilde{\psi}}\left|\cos\psi + \cos\left(\frac{2\pi(K+1)}{f_s} + \psi\right)\right| d\psi\right].
\end{aligned}$$

Plugging this result into (7), we get after some algebra

$$\bar{e}_x(f_s) \approx \frac{f_s}{2}\left[\cos\left(\frac{K\pi}{f_s}\right)\left(1-\sin\left(\frac{(K+1)\pi}{f_s}\right)\right)\right.$$
$$\left.+\cos\left(\frac{(K+1)\pi}{f_s}\right)\left(\sin\left(\frac{K\pi}{f_s}\right)-1\right)\right]. \tag{9}$$

Finally, the above result can be greatly simplified by the use of the common approximations "$\sin u \approx u$" and "$1-\cos u \approx u^2/2$" for small u's. If we assume that $\pi/f_s \ll 1$, we have then $|\pi/2 - K\pi/f_s| \ll 1$ too and, therefore, (9) reduces to

$$\bar{e}_x(f_s) \approx \frac{\pi^3}{16 f_s^2}(2(K+1)-f_s)(f_s-2K). \tag{10}$$

As it can be seen from this last equation, the model results in a parabolic approximation of $\bar{e}_x(f_s)$ on each sampling frequency interval of the form $\{[2k, 2(k+1)], k \in \mathbb{N}\}$, thus justifying the decay of $\bar{e}_x(f_s)$ around frequencies that match even numbers. Moreover, the model accounts for the "$1/f_s^2$" tendency reported above, as evidenced by the prefactor, and it is also equal to $\bar{e}_x(f_s)$ for every integer sampling frequency.[b]

The final approximation (10) is plotted in Fig. 2 (right diagram). It is worth noticing that the approximation holds well for the whole frequency range.

3. Generalization Beyond Tones

To address properly the sampling issue, we first have to define some minimum requirements on the sampling parameters for a continuous-time signal to be processed by EMD. As extrema play a major role in the sifting process, a natural requirement would be for a discrete-time signal to keep as many extrema as does its continuous-time counterpart. In fact, losing one extremum during the sampling process usually means losing a pair of maximum/minimum, which in turn means losing one local oscillation for the EMD. To ensure that there is no loss of extrema, the minimum requirement is for *the sampling period to be at most one half of the minimum distance between extrema* in the signal. Moreover, the sampling period should be longer than any interval where the signal is constant. In all the following, we will implicitly consider that these requirements are met.[c]

[b]Unlike what is said in Ref. 3, the corresponding model in this paper is also exact under the very same conditions, up to a missing $\sqrt{2}$ factor.

[c]It is worth noticing that this requirement is completely independent from Shannon's sampling criterion for band-limited signals: indeed, a band-limited signal can have arbitrary close extrema, whatever its frequency band. For instance, $t \mapsto (1-\epsilon)\sin \epsilon f t - \epsilon \sin f t$ has two extrema at $\pm\sqrt{2\epsilon}/f$ for $\epsilon \ll 1$.

3.1. *A bound on the sampling error for the elementary sifting operator*

Given a continuous-time signal $x(t)$ with a minimum distance Δ between its extrema and constant interval shorter than $\Delta/2$, we will consider as before its discretized versions $\{x_{f_s,\varphi}[n] = x(n/f_s+\varphi), n \in \mathbb{Z}\}$, with the aim of characterizing the behavior of their EMD as a function of the sampling frequency $f_s > 2/\Delta$. More particularly, we will be mainly interested in the deviation between the sampled IMFs and the theoretical, continuous-time ones. When dealing with sinusoidal signals however, we based ourselves on three hypotheses (see Sec. 2.2). Among these, the second one, saying that the first IMF is obtained through a unique sifting step, is a fair approximation for sinusoidal signals but becomes a really strong assumption for more general cases. Indeed, some extrema pairs are likely to appear after any iteration of the sifting process, thus compelling us to consider all the sifting steps. This unfortunately brings about two major issues to the analysis of the influence of sampling:

1. If an extrema pair appears at some point in the sifting process for a given set of sampling parameters, there is no guarantee that a similar extrema pair will ever appear for another set, even for same sampling frequencies and different phases. Moreover, the appearance of an extrema pair for a given set of sampling parameters seems rather unpredictable.
2. We generally do not know how many sifting steps are to be performed to extract the first IMF. Moreover, as this is generally decided by a test within the sifting loop, the precise number of iterations may depend on the analyzed discrete signal and therefore on the sampling parameters.

Because of these cumbersome issues, we will mainly focus on the effect of sampling on *one sifting step only*, or on what we refer to as "the sifting elementary operator" (thereafter denoted $\mathcal{S}$) corresponding to the operation of subtracting to a signal the mean of its envelopes. More precisely, we will investigate the case of a simplified elementary operator for which we can derive an upper bound for the sampling effects. The obtained results will then be assessed by simulations using the original operator.

3.1.1. *Model*

We start off with analyzing the effects of sampling on the extrema. If t_0 is the position of a local maximum in $x(t)$, the condition $f_s > 2/\Delta$ ensures that there is also a maximum in $x_{f_s,\varphi}[n]$ for n such that $|n/f_s + \varphi - t_0| < 1/f_s$, i.e., that the closest sampling point — either on the right or on the left — of the continuous-time maximum is a maximum for the sampled signal. More precisely, we can define the index of the extremum in the sampled signal as the one (or one of the two) such that $n/f_s + \varphi \in I_0 \equiv [t_0 - a, t_0 + b]$ with $a, b > 0$, $a + b = 1/f_s$, and $x(t_0 - a) = x(t_0 + b)$. We can thus define an uncertainty in abscissa $\Delta^{(0)}_{\text{abs}}$ as the maximum deviation, in abscissa, between the continuous-time extremum and the discrete-time

extremum: $\Delta^{(0)}_{\text{abs}} = \max\{a, b\}$. The corresponding uncertainty in ordinates can then be defined as: $\Delta^{(0)}_{\text{ord}} = |x(t_0) - x(t_0 - a)| = |x(t_0) - x(t_0 + b)| = \min\{|x(t_0) - x(t_0 + \Delta^{(0)}_{\text{abs}})|, |x(t_0) - x(t_0 - \Delta^{(0)}_{\text{abs}})|\}$.

Taking these uncertainties into account, the next step in the analysis is to evaluate their impact on the envelopes $e_{\min}(t)$ and $e_{\max}(t)$. Usually, these envelopes are computed using a cubic spline interpolation.[1,2] In our model however, we will use *piecewise linear interpolation* (this is the only simplification we consider for the elementary operator $\mathcal{S}$). The reason for this is simply that the value of a cubic spline interpolation between two knots depends not only on a few knots around but also on all the knots defining the interpolation. In this context, calculating an uncertainty on the value of the interpolation at a specific position, given uncertainties on all the knots, is rather complicated. It turns out that evaluation is much simpler with a piecewise linear interpolation, while guaranteeing that the obtained uncertainties generally match the observations.

If we then consider two consecutive maxima $(t_0, x(t_0))$ and $(t_1, x(t_1))$ in the continuous-time signal, the corresponding maxima in the sampled signal are located within the rectangular boxes $\{[t_i - \Delta^{(i)}_{\text{abs}}, t_i + \Delta^{(i)}_{\text{abs}}] \times [x(t_i) - \Delta^{(i)}_{\text{ord}}, x(t_i)]; i = 0, 1\}$ (see Fig. 3). In this context, it is clear that the largest error for the envelope is obtained for the thick dash–dot line case. Integrating this error over the range $[t_0, t_1]$ (corresponding to the shaded surface in Fig. 3), we get over this range a bound (referred to as $\delta e_{\max}(t)$) on the sampling error for the upper envelope $e_{\max}(t)$:

$$\int_{t_0}^{t_1} |\delta e_{\max}(t)| dt \leq \frac{(t_1 - t_0)(\Delta^{(0)}_{\text{ord}} + \Delta^{(1)}_{\text{ord}})}{2} + (t_1 - t_0)\frac{|x(t_1) - x(t_0) - \Delta^{(1)}_{\text{ord}} + \Delta^{(0)}_{\text{ord}}|(\Delta^{(1)}_{\text{abs}} + \Delta^{(0)}_{\text{abs}})}{2(t_1 - t_0 - |\Delta^{(1)}_{\text{abs}} - \Delta^{(0)}_{\text{abs}}|)},$$

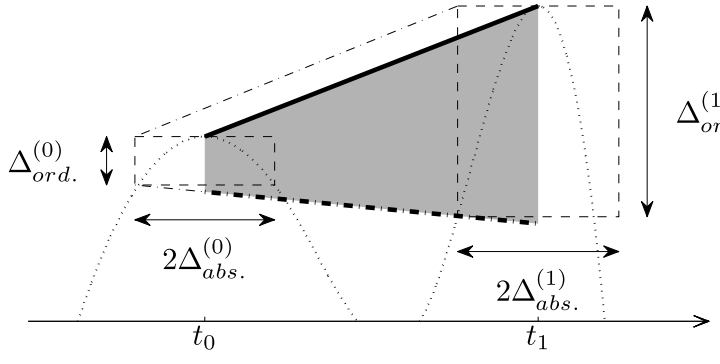

Fig. 3. Evaluating the uncertainty for the envelopes. For both maxima, the dashed boxes delimit the areas where the corresponding maxima in the sampled signal can be located. The thick plain line stands for the interpolation (piecewise linear in the model) based on the extrema in the continuous-time signal. Then the dash–dot lines delimit the area where the interpolation based on the extrema in the sampled signal can be located. Finally, the thick dash–dot line stands for the case that leads to the largest error.

which leads in turn to the looser bound

$$\begin{aligned}\int_{t_0}^{t_1} |\delta e_{\max}(t)|dt \leq (t_1 - t_0) \cdot \frac{\Delta_{\text{ord}}^{(0)} + \Delta_{\text{ord}}^{(1)}}{2} \\ + |x(t_1) - x(t_0)| \cdot \frac{\Delta_{\text{abs}}^{(1)} + \Delta_{\text{abs}}^{(0)}}{2} \\ + \frac{t_1 - t_0}{t_1 - t_0 - |\Delta_{\text{abs}}^{(1)} - \Delta_{\text{abs}}^{(0)}|} \cdot \frac{\Delta_{\text{abs}}^{(1)} + \Delta_{\text{abs}}^{(0)}}{2} \cdot |\Delta_{\text{ord}}^{(1)} - \Delta_{\text{ord}}^{(0)}| \\ + \frac{|\Delta_{\text{abs}}^{(1)} - \Delta_{\text{abs}}^{(0)}|}{t_1 - t_0 - |\Delta_{\text{abs}}^{(1)} - \Delta_{\text{abs}}^{(0)}|} \cdot |x(t_1) - x(t_0)|. \qquad (11)\end{aligned}$$

In the last formula, the first term can be read as the average uncertainty caused by the uncertainties in ordinate only, its amplitude depending only on the behavior of the signal around its extrema. This contrasts with the second term which, depending on the uncertainties in abscissa, does not only depend on the behavior of the signal around its extrema, but also on the relative amplitudes of successive extrema. If the analyzed signal is, e.g., an amplitude modulated (AM) sinusoidal signal, then the amplitude of the first term will only depend on the sampling frequency and on the frequency of the carrier, while the second one will depend on the frequency and amplitude of the modulation too. Finally, the last terms, depending on both uncertainties, are generally much smaller than the first two ones and can therefore be neglected in most cases.

If we compute the bound (11) on each range delimited by two consecutive maxima, we obtain a bound for the L_1-norm of the sampling related effects on the upper envelope. Repeating the same operation for the lower envelope then results in a bound on the error for the mean of the envelopes, which is simply the mean of the bounds on each envelope. Finally, this bound is also valid for the elementary operator defined as the difference between the signal and the mean of the envelopes.

3.1.2. *Estimating the parameters from the signal*

Given a signal $x(t)$, computing the upper bound (11) requires only a limited set of parameters (namely, the positions $(t_i, x(t_i))$ and the uncertainties $\Delta_{\text{abs}}^{(i)}$ and $\Delta_{\text{ord}}^{(i)}$ for each extremum) that are rather easy to measure in continuous-time. However, if we only have a discrete version of the signal, some of these parameters cannot be evaluated without prior additional information. Indeed, the $(t_i, x(t_i))$ can be estimated by the corresponding extrema values in the discrete signal: $\hat{t}_i = n_i/f_s + \varphi$ and $\hat{x}_i = \widehat{x(t_i)} = x_{f_s,\varphi}[n_i]$, where n_i is the index of the ith extremum in the discrete signal. In these estimates the time instants t_i are estimated with a precision of order $1/f_s$. This unfortunately implies that the uncertainties in abscissa $\Delta_{\text{abs}}^{(i)} \in [1/2f_s, 1/f_s[$ cannot be estimated with a decent precision, thus constraining us to use the upper bound $1/f_s$ as a default value for all extrema. Similarly, the $\Delta_{\text{ord}}^{(i)}$

cannot be estimated from the sampled signal only but, on the other hand they may be if we have some additional information on the behavior of the signal around its extrema. A natural way to proceed is to make a regularity assumption on the signal: if we, e.g., require the signal to be twice continuously differentiable, then we can use a second-order Taylor expansion to estimate the behavior of the signal around its extrema. We can this way use the parabolic approximation $x(t)-x(t_i) \approx \frac{1}{2}(t-t_i)^2 x''(t_i)$, which leads to $\Delta_{\mathrm{ord}}^{(i)} \approx \frac{1}{2}|x''(t_i)|/f_s^2$, where the second derivatives $x''(t_i)$ can themselves be estimated using finite difference operators at the extrema of the sampled signal, leading to $\hat{x}_i''$. Putting these approximations back into (11) results in an estimate of the maximum sampling error over the range $[t_i, t_{i+1}]$ for the upper envelope:

$$\int_{t_i}^{t_{i+1}} |\delta e_{\max}(t)| dt \leq \frac{(\hat{t}_{i+1}-\hat{t}_i)|\hat{x}_i'' + \hat{x}_{i+1}''|}{4f_s^2} + \frac{|\hat{x}_{i+1}-\hat{x}_i|}{f_s} + \frac{|\hat{x}_{i+1}''-\hat{x}_i''|}{2f_s^3}.$$

We are thus led to the central result of this paper which is the existence of an upper bound for the L_1-norm of the sampling error for the elementary operator $\delta\mathcal{S}$ of the form

$$\|\delta\mathcal{S}x\|_1 \leq \frac{\lambda}{f_s} + \frac{\mu}{f_s^2} + \frac{\nu}{f_s^3}, \tag{12}$$

where the integration for the L_1-norm essentially extends to the observation interval of the analyzed signal and with

$$\lambda = \frac{1}{2}\left(\sum_i \left|\hat{x}_{i+1}^m - \hat{x}_i^m\right| + \sum_i \left|\hat{x}_{i+1}^M - \hat{x}_i^M\right|\right), \tag{13}$$

$$\mu = \frac{1}{8}\left(\sum_i \left(\hat{t}_{i+1}^m - \hat{t}_i^m\right)\left|\hat{x}_i^{m\prime\prime} + \hat{x}_{i+1}^{m\prime\prime}\right| + \sum_i \left(\hat{t}_{i+1}^M - \hat{t}_i^M\right)\left|\hat{x}_i^{M\prime\prime} + \hat{x}_{i+1}^{M\prime\prime}\right|\right), \tag{14}$$

$$\nu = \frac{1}{4}\sum_i \left|\hat{x}_{i+1}^{m\prime\prime} - \hat{x}_i^{m\prime\prime}\right| + \left|\hat{x}_{i+1}^{M\prime\prime} - \hat{x}_i^{M\prime\prime}\right|, \tag{15}$$

where superscripts m and M refer to minima and maxima, respectively.

Remark. Our previous studies showed that, in the specific case of sinusoidal signals, the sampling error is upper bounded by a function proportional to f_s^{-2}.[3] The bound (12) obtained here generalizes this result since the parameters λ and ν are simply zero in the sinusoidal case. Nevertheless, the μ coefficient computed with (14) for sinusoidal signals leads to a bound that is looser than the one we obtained in Ref. 3, and there are two reasons for this. First, a sinusoidal signal is symmetric with respect to each extremum: therefore, the uncertainty in abscissa Δ_{abs} can be reduced to $1/(2f_s)$, leading to the reduced parameter values: $\lambda' = \lambda/2$, $\mu' = \mu/4$, and $\nu' = \nu/8$. Second, there is generally a partial compensation between the errors associated to the f_s^{-2} terms coming from the upper and the lower envelope. This can be easily controlled for the sinusoidal case, allowing a bound reduced by one half and thus in agreement with our former results.

3.1.3. *Validation*

To assess the performance of the upper bound model (12), we need to measure the difference between the continuous-time EMD of a continuous-time signal and the discrete-time EMDs of sampled versions of the same signal for various sampling parameters. To that end, we performed a set of simulations using synthetic piecewise polynomial signals. As the extrema of a polynomial of order less than 4 are analytically known, the continuous-time EMD of a piecewise polynomial can be defined properly. At first, we will not compare IMFs obtained from the continuous-time signal with those obtained from sampled signals but we will restrain to the first IMF obtained with a unique sifting iteration. Thus, we do not really compare outputs of EMD but only outputs of the elementary operator, as for the model. The overall methodology can be summarized by the following procedure:

1. Synthetize a continuous-time piecewise polynomial oscillating signal $x(t), t \in [0, L]$ such that the minimum distance between two extrema is greater than 2, and L is such that the number of extrema is large enough to neglect border effects.
2. Apply the continuous-time elementary operator: $y_\infty(t) \equiv (\mathcal{S}x)(t)$.
3. Define the sampled signals: $x_{f_s,\varphi}[n] \equiv x\left(\frac{n}{f_s} + \varphi\right)$ for $0 \leq n \leq N(f_s) \equiv \lfloor L f_s \rfloor - 1$ and $0 \leq \varphi < \frac{1}{f_s}$ (where $\lfloor \cdot \rfloor$ stands for the integer part).
4. Apply the elementary sifting operator to each sampled signal: $y_{f_s,\varphi}[n] \equiv (\mathcal{S}x_{f_s,\varphi})[n]$.
5. For each sampling parameters set (f_s, φ), compute the sampling error measure[d]

$$e(f_s, \varphi) \equiv \frac{1}{N(f_s)+1} \sum_{n=0}^{N(f_s)} \left| y_{f_s,\varphi}[n] - y_\infty\left(\frac{n}{f_s} + \varphi\right)\right|. \tag{16}$$

The test signals we used are piecewise cubic polynomials obtained through interpolation of a random set of extrema. The main property of the underlying model is that it ensures that the minimum distance between extrema is set by a parameter Δ. The details are of lesser importance as the results seem to be weakly dependent on the model.

Simulation results are plotted in Fig. 4 for two representative examples. As it can be seen on the figure, the behavior of the bound as a function of the sampling frequency can generally be divided into two areas: for lower sampling frequencies, the bound usually behaves like f_s^{-2} whereas, for higher frequencies, it behaves like f_s^{-1} (see Fig. 4(b)). There are specific cases however where the f_s^{-1} area does not exist, since the coefficient λ given by (13) is typically zero when all the maxima/minima have the same amplitude (see Fig. 4(a)). This twofold behavior also applies to

[d]The choice made here of a l_1-norm is not critical, other norms leading to similar results.

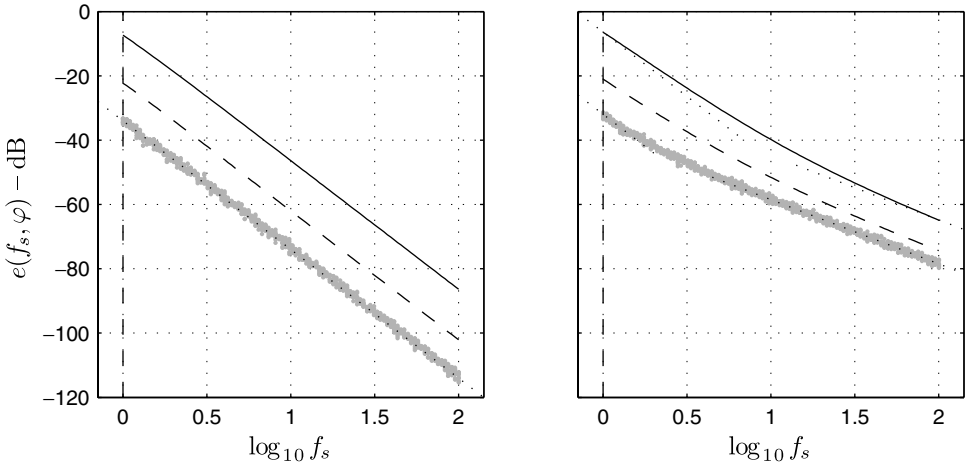

Fig. 4. Sampling error and bound estimate as a function of the sampling frequency for the elementary operator. On both graphs, each gray dot stands for a measure of sampling error according to (16). For each sampling frequency and phase, a bound is also estimated according to (12) from the downsampled signal: the mean of these with respect to the phase is plotted against sampling frequency as a solid line. The dashed line corresponds to the average sampling error (18) computed with $\alpha = 0.7$. Cases (a) and (b) correspond to rather close signals, the difference being that (a) has constant maxima/minima amplitudes while (b) has random maxima/minima values centered around 1/−1 with variance 0.1. Asymptotic f_s^{-1} or f_s^{-2} behaviors are evidenced by dotted lines.

the measured sampling error, but either the f_s^{-1} or the f_s^{-2} area can be missing. Moreover, when both are present, the critical sampling frequency delimiting these areas is generally not the same as the corresponding critical frequency for the bound. The evolution of the bound however usually gives a fair outline for the evolution of the sampling error. Besides, the f_s^{-3} behavior that we could expect from (12) has never been observed distinctly.

Quantitatively, the sampling error measured in our simulations is always rather far from the bound. The latter usually is around 12 dB above in the f_s^{-1} area and 25 dB in the f_s^{-2} area. This discrepancy comes mainly from the fact that the bound is obtained by considering a worst case error everywhere whereas this worst case is rather improbable. To relate the bound to the simulation results, we can consider a variation on the model giving an average value instead of an upper bound for the errors in abscissa and ordinate for each extremum. Basically, we can take averaged values of the errors with respect to the sampling phase:

$$\forall\, i, \quad \bar{\Delta}^{(i)}_{\text{abs}} = \mathbb{E}_\varphi\{|t_i - (n_i f_s + \varphi)|\},$$
$$\bar{\Delta}^{(i)}_{\text{ord}} = \mathbb{E}_\varphi\{|x(t_i) - x_{f_s,\varphi}[n_i]|\},$$

where n_i refers to the index of the extremum corresponding to $(t_i, x(t_i))$ in the discrete signal. In order to estimate these quantities, we can use the local parabolic

approximation again, thus leading to:

$$\bar{\Delta}_{\text{abs}}^{(i)} = \frac{\Delta_{\text{abs}}^{(i)}}{2},$$

$$\bar{\Delta}_{\text{ord}}^{(i)} = \frac{\Delta_{\text{ord}}^{(i)}}{3}.$$

Now, even with this average model, the sampling error estimate still lies several dB above the simulation results, typically about 10 dB in the f_s^{-2} area and 4 dB in the f_s^{-1} area. One reason for this is that we use $1/f_s$ for the uncertainties in abscissa while we know that the actual uncertainty with our test signals is generally smaller than $0.7/f_s$. If we had used an average value α/f_s, $1/2 \leq \alpha < 1$ (instead of $1/f_s$), then the three parameters λ, μ, and ν defined by Eqs. (13), (14), and (15) would have been replaced by:

$$\lambda' = \alpha\lambda, \quad \mu' = \alpha^2\mu \quad \text{and} \quad \nu' = \alpha^3\nu. \tag{17}$$

Combining these with the former average model, we get the following estimate for the average sampling error (ASE):

$$ASE = \frac{\alpha\lambda}{2} + \frac{\alpha^2\mu}{3} + \frac{\alpha^3\nu}{6}. \tag{18}$$

The average model with corrected uncertainties in abscissa is much closer to the simulation results but still some dB above. There are mainly two reasons for the remaining error. First, there is a deviation coming from the use of a parabolic approximation around the extrema to compute the uncertainties in ordinate. Second, the sampling error on the upper envelope generally partially (sometimes totally) compensates for the sampling error on the lower envelope, whereas the two corresponding bounds are just summed in the model. Moreover, the compensation is greater in the f_s^{-2} area because the f_s^{-2} term in (12) corresponds to deviations of the ordinates of the extrema which are always negative for maxima and positive for minima. Therefore, the deviations coming from both envelopes always compensate at least partially for each other while they are summed in the model. Unfortunately, the magnitude of the compensation cannot be estimated properly from the discrete signal because it would require to know the abscissa of the extrema with a precision better than the sampling period.

3.2. *Consequences on the EMD*

In order to study the influence of sampling on a complete EMD we can as before compare outputs obtained from the continuous-time signal to others obtained from sampled versions of that signal. The evaluation procedure is therefore very close to that used in the previous section, the only differences being that we do not restrain to the first IMF any more and that the IMFs are now obtained with a variable number of sifting iterations, possibly depending on the sampling parameters. Simulation results based on the signal used for Fig. 4(b) are presented Fig. 5. The stopping

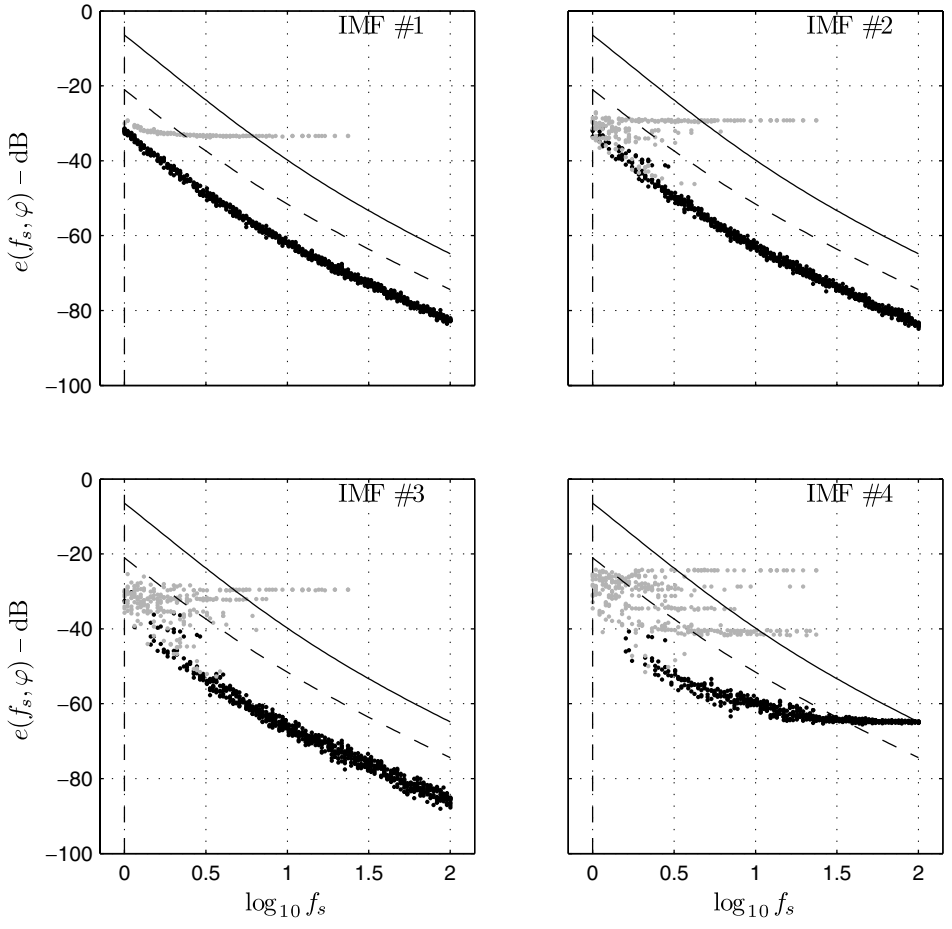

Fig. 5. Sampling error and bound estimate as a function of the sampling frequency for the first four IMFs. On the four graphs, each dot stands for a measure of sampling error according to (16). Black dots stand for cases where the numbers of iterations used to compute the IMF and all the previous ones are the same as for the continuous-time signal. Gray dots stand for cases where some of these numbers of iterations differ. The bound (12) and the average sampling error (18) computed from the sampled signal are plotted as solid and dashed lines, respectively. The signal used for this example is the same as for Fig. 4(b).

criterion used for sifting is the default stopping criterion in our EMD `MATLAB` code (available at Ref. 6) which is[e]

$$\forall\, t, \quad \frac{|e_{\max}(t) + e_{\min}(t)|}{|e_{\max}(t) - e_{\min}(t)|} < \epsilon, \tag{19}$$

with $\epsilon = 0.05$ by default.

[e]The stopping criterion is in fact a bit more complicated[2] but its behavior in this test situation is mostly given by (19).

If we first look at the first IMF, we can see that for all sampling frequencies there is a set of sampling phases for which the deviation between the first IMF obtained from the continuous-time signal and that obtained from the sampled signal behaves almost as the corresponding deviation for elementary operators. More precisely, the deviation between IMFs is even a bit smaller, which we cannot explain by our simple model. However, the fact that it does not increase is interesting as it implies that most of the deviation related to sampling results from the first sifting iteration. If we take into account the numbers of iterations, it appears that these situations where the deviation is similar to that observed for the elementary operator in fact correspond to cases where the number of sifting iterations used to compute the first IMF is exactly the same (3 here) as the one used for the continuous-time signal. On the other hand, when the number of iterations is different, the deviation is much larger. The amplitude of the latter is typically related to the deviation between an IMF obtained with n iterations and $n+1$ iterations which is controlled by ϵ. As a matter of fact, we observe that these larger deviations are generally reduced when ϵ is reduced but it is not always true since the differences between numbers of iterations are likely to be greater, which may lead to larger deviations.

The deviations between continuous-time and discrete-time for the next IMFs show some similarities with the case of the first IMF. Indeed, we observe that when the number of iterations used to compute an IMF and all the previous ones are identical to those used for the continuous-time signal, then the deviation is similar to that observed for the elementary operator. As for the first IMF, these deviations are in fact a bit smaller and they are even smaller for the second and third IMFs. On the other hand, the deviation increases for the fourth IMF in our specific case. Once again, these deviations between successive IMFs cannot be explained by our simple model. However, as for the first IMF, the fact that the deviation between continuous-time and discrete-time IMFs does not increase with the index of the IMF implies that most of the deviation comes from the first IMF. The explanation for this is straightforward: the IMFs with indices larger than one are extracted from the difference between the signal and the first IMF which oscillates more slowly than the signal itself and is therefore less sensitive to sampling. Moreover, this also explains why the deviation is close to that observed for the first IMF since the signal from which the next IMFs are extracted already contains that deviation. However, when the number of iterations differ for the observed IMF or for any previous ones, the deviations become much larger similarly to what has been observed for the first IMF. These much larger deviations are even sometimes larger than for the first IMF which can be explained by an accumulation of deviations coming from the observed IMF and the previous ones. Moreover, the most important feature is maybe that these situations with larger deviations are even more common when the index of the observed IMF gets larger which implies that fewer situations can be described by our model.

4. Conclusion

The question of the influence of sampling on EMD has been addressed here in some detail, from the derivation of theoretical results in simplified cases to the observation of effective behaviors in more realistic situations. The existence of bounds on possible errors due to sampling allows now for a quantitative approach which goes beyond the qualitative precautionary principle of only applying EMD to "sufficiently oversampled" data. However, the impact of sampling on the EMD is not fully understood. There are, e.g., intriguing phenomena where the deviation resulting from sampling diminishes when the sifting process is iterated. Moreover, the deviations related to sampling induce deviations in the numbers of iterations which in turn lead to larger deviations. This problem is unfortunately unavoidable if the numbers of iterations depend on the signal. On the other hand, its importance may seem marginal since the IMFs are obviously defined up to some uncertainty related to the stopping criterion and since the amplitude of those larger deviations is often close to that uncertainty. However, these deviations can also imply that some extrema appear in some situations and not in others. This may especially be a problem if one is interested in a specific localized oscillation because its appearance in a specific IMF may depend on the sampling parameters.

References

1. N. E. Huang, Z. Shen, S. R. Long, M. L. Wu, H. H. Shih, Q. Zheng, N. C. Yen, C. C. Tung and H. H. Liu, The empirical mode decomposition and Hilbert spectrum for nonlinear and non-stationary time series analysis, *Proc. Roy. Soc. London A* **454** (1998) 903–995.
2. G. Rilling, P. Flandrin and P. Gonçalves, On empirical mode decomposition and its algorithms, in *IEEE-EURASIP Workshop on Nonlinear Signal and Image Processing NSIP-03* (Grado (I), 2003).
3. G. Rilling and P. Flandrin, Sur la Décomposition Modale Empirique des signaux échantillonnés, in *Proc. 20^e Coll. GRETSI sur le Traitement du Signal et des Images* (Louvain-la-Neuve (B), 2005), pp. 755–758.
4. G. Rilling and P. Flandrin, On the influence of sampling on the empirical mode decomposition, in *IEEE Int. Conf. Acoust. Speech and Signal Proc.* (Toulouse (F), 2006), DOI: 10.1109/ICASSP.2006.1660686.
5. M. Stevenson, M. Mesbah and B. Boashash, A sampling limit for the empirical mode decomposition, in *Proc. Int. Symp. Signal Proc. and its Appl. ISSPA-05* (Sydney (A), 2005), pp. 647–650.
6. http://perso.ens-lyon.fr/patrick.flandrin/emd.html.